Asian Journal of Chemistry; Vol. 26, No. 5 (2014), 1297-1300

ASIAN JOURNAL OF CHEMISTRY

http://dx.doi.org/10.14233/ajchem.2014.17213

Synthesis and Spectroscopic Properties of Superparamagnetic Iron Oxide Nanoparticle/ $CaWO_4:Er^{3+}, Yb^{3+}$ Composites by Microwave-Assisted Metathetic Method†

CHANG SUNG LIM

Department of Advanced Materials Science & Engineering, Hanseo University, Seosan 356-706, Republic of Korea

Corresponding author: Tel/Fax: +82 416601445; E-mail: cslim@hanseo.ac.kr

Published online: 1 March 2014; AJC-14754

Er^{3+}/Yb^{3+} co-doped $CaWO_4$($CaWO_4:Er^{3+}/Yb^{3+}$) composites with superparamagnetic iron oxide nanoparticles (SPIONs) were successfully synthesized by a cyclic microwave-assisted metathetic method followed by heat-treatment. The microstructure exhibited well-defined and homogeneous morphology with the $CaWO_4:Er^{3+}/Yb^{3+}$ particle size of 1-2 μm and Fe_3O_4 particle size of 0.1-0.5 μm. The Fe_3O_4 particles were self-preferentially crystallized and immobilized on the surface of $CaWO_4:Er^{3+}/Yb^{3+}$ particles. The synthesized SPION/$CaWO_4:Er^{3+}/Yb^{3+}$ composites were characterized by X-ray diffraction, scanning electron microscopy and energy-dispersive X-ray spectroscopy. Spectroscopic properties were examined using Raman spectroscopy.

Keywords: SPIONs, $CaWO_4:Er^{3+}/Yb^{3+}$, Microwave-assisted metathetic synthesis, SEM/EDS, Raman spectroscopy.

INTRODUCTION

Superparamagnetic iron oxide nanoparticles (SPIONs) incorporated into photoluminescent composites containing two different functionalities could provide novel characteristics *via* the integration of fluorescent and magnetic properties, offering new potential in a wide range of applications in biomedical systems, such as targeted drugs, diagnostics, therapeutics and bio-imaging[1-3]. The particles of rare-earth-doped upconversion of $CaWO_4$ molybdate which shows a Scheelite-type structure with unit cell parameters a = b = 5.2425 Å and c = 11.3715 Å[4], are relatively stable in the air and have stable physical and chemical properties, low excitation threshold energy and low-cost productivity. Recently, several processes have been developed to increase the applications of rare-earth-doped $CaWO_4$ prepared using a range of processes including solid-state reactions[5,6], the sol-gel method[7], the hydrothermal method[8,9], the combustion method[10], the solvothermal route[11] and the sonochemical method[12]. For practical application of photoluminescence in such products as lasers, three-dimensional displays, light-emitting devices and biological detectors, features such as homogeneous particle size distribution and morphology need to be well defined.

The cyclic microwave-assisted metathetic (MAM) synthesis of materials is a simple and cost-effective method that provides a high yield with an easy scale-up and it is emerging as a viable alternative approach for the synthesis of high-quality novel inorganic materials in short time periods[13]. In this study, the Er^{3+}/Yb^{3+} co-doped $CaWO_4$ ($CaWO_4:Er^{3+}/Yb^{3+}$) and Er^{3+}/Yb^{3+} co-doped $CaWO_4$ with SPIONs (SPION/$CaWO_4:Er^{3+}/Yb^{3+}$) composites were synthesized by the cyclic microwave-assisted metathetic method followed by heat-treatment. The synthesized $CaWO_4:Er^{3+}/Yb^{3+}$and SPION/$CaWO_4:Er^{3+},Yb^{3+}$ composites were characterized by X-ray diffraction (XRD), scanning electron microscopy (SEM) and energy-dispersive X-ray spectroscopy (EDS). Spectroscopic properties have been investigated by Raman spectroscopy.

EXPERIMENTAL

Appropriate stoichiometric amounts of $CaCl_2$, $ErCl_3·6H_2O$, $YbCl_3·6H_2O$, $Na_2WO_4·2H_2O$, 5-nm-sized Fe_3O_4 nanoparticles and ethylene glycol of analytic reagent grade were used to prepare the $CaWO_4:Er^{3+},Yb^{3+}$ and SPION/$CaWO_4:Er^{3+},Yb^{3+}$ compounds. To prepare $CaWO_4:Er^{3+}/Yb^{3+}$, 0.8 mol % $CaCl_2$ with 0.02 mol % $ErCl_3·6H_2O$ and 0.18 mol % $YbCl_3·6H_2O$ and 1 mol % $Na_2WO_4·2H_2O$ were dissolved in 30 mL of ethylene glycol. To prepare SPION/$CaWO_4:Er^{3+},Yb^{3+}$, 0.2 mol % $CaCl_2$ with 0.02 mol % $ErCl_3·6H_2O$ and 0.18 mol % $YbCl_3·6H_2O$ and 1 mol % $Na_2MoO_4·2H_2O$ with 0.5 mol % Fe_3O_4 were

†Presented at The 7th International Conference on Multi-functional Materials and Applications, held on 22-24 November 2013, Anhui University of Science & Technology, Huainan, Anhui Province, P.R. China

dissolved in 30 mL ethylene glycol. The solutions were mixed and adjusted to pH 9.5 using NaOH. The solutions were stirred at room temperature. Then, the mixtures were transferred into 120 mL Teflon vessels. Each Teflon vessel was placed into a microwave oven operating at the frequency of 2.45 GHz with the maximum output power of 1250 W for 23 min. The working cycle of the microwave-assisted metathetic reaction was been controlled precisely between 30 s on and 30 s off for 8 min, followed by a further treatment of 30 s on and 60 s off for 15 min. Ethylene glycol was evaporated slowly at its boiling point. Ethylene glycol is a polar solvent at its boiling point of 197 ºC and it is a good candidate for the microwave process. The resulted powder samples were treated with ultrasonic radiation and washed many times with hot distilled water. The white precipitates were collected and dried at 100 ºC in a drying oven. After this, the final products were heat-treated at 600 ºC for 3 h.

The phase composition of final powder products formed after the cyclic MAM reaction and following heat-treatment was identified using XRD (D/MAX 2200, Rigaku, Japan). The microstructures and surface morphologies of the $CaWO_4:Er^{3+}/Yb^{3+}$ and $SPION/CaWO_4:Er^{3+}/Yb^{3+}$ composites were observed using SEM/EDS (JSM-5600, JEOL, Japan). Their PL spectra were recorded at room temperature using a spectrophotometer (Perkin Elmer LS55, UK). Raman spectroscopy measurements were performed using a LabRam HR (Jobin-Yvon, France) device. The 514.5 nm line of an Ar-ion laser was used as an excitation source and the power on the samples was kept at 0.5 mW.

RESULTS AND DISCUSSION

Fig. 1 shows the XRD patterns of (a) pure $CaWO_4$ (JCPDS 72-1624) and (b) the synthesized $SPION/CaWO_4:Er^{3+}/Yb^{3+}$ particles. All the diffraction peaks were assigned to the tetragonal-phase $CaWO_4$ with a Scheelite-type structure and Fe_3O_4, which were in good agreement with the crystallographic data of $CaWO_4$ (JCPDS 72-1624) and Fe_3O_4 (JCPDS 19-0629). The diffraction peaks marked with asterisk are related to Fe_3O_4. The result confirms that the $SPION/CaWO_4:Er^{3+},Yb^{3+}$ composites can be prepared using the cyclic MAM route. The post-synthesis heat-treatment plays an important role in forming well-defined crystallized micromorphology. To achieve such morphology, the $SPION/CaWO_4:Er^{3+},Yb^{3+}$ composites need to be heated at 600 ºC for 3 h. This suggests that the cyclic MAM route, in combination with subsequent heat-treatment, is a suitable way for the formation of $SPION/CaWO_4:Er^{3+},Yb^{3+}$ polycrystalline composites with well developed high-intensity peaks from the (101), (112) and (204) planes, which are the major peaks[4] of $CaWO_4$.

The SEM image of the synthesized $SPION/CaWO_4:Er^{3+},Yb^{3+}$ composite is shown in Fig. 2. The as-synthesized sample has a well-defined and homogeneous morphology with the $CaWO_4:Er^{3+},Yb^{3+}$ particle size of 1-2 μm and Fe_3O_4 particle size of 0.1-0.5 μm, respectively. The Fe_3O_4 particles were self-preferentially crystallized and immobilized on the surface of big $CaWO_4:Er^{3+},Yb^{3+}$ particles.

The incorporation of Fe_3O_4 nanoparticles to the $CaWO_4:Er^{3+},Yb^{3+}$ compound particles can be successfully achieved

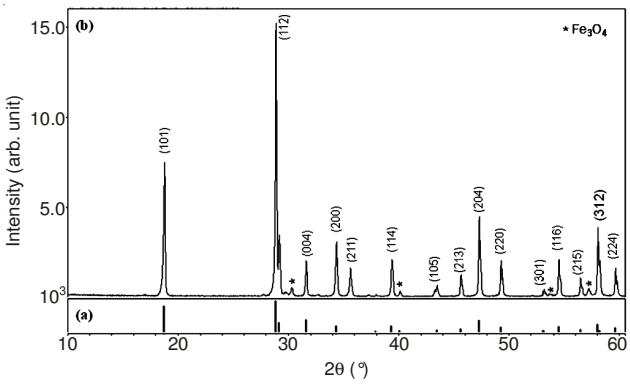

Fig. 1. XRD pattern of (a) pure $CaWO_4$ and (b) the synthesized $SPION/CaWO_4:Er^{3+},Yb^{3+}$ composites

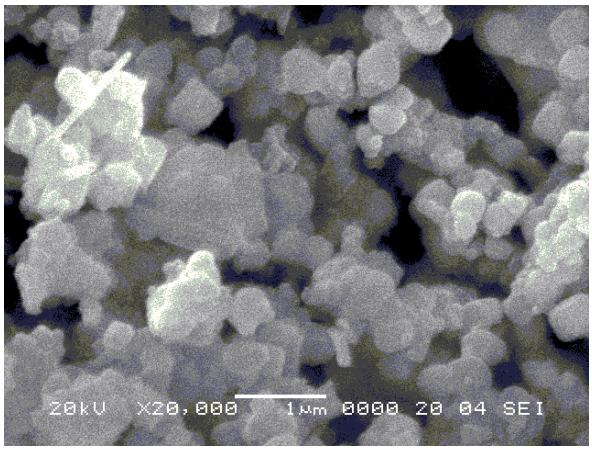

Fig. 2. A SEM image of the synthesized $SPION/CaWO_4:Er^{3+},Yb^{3+}$ composites

using the cyclic MAM method. The MAM reactions, such as $CaCl_2 + Na_2WO_4 \rightarrow CaWO_4 + 2NaCl$, involve the exchange of atomic/ionic species, in which the driving force is the exothermic reaction accompanying the formation of NaCl[13]. The $SPION/CaWO_4:Er^{3+},Yb^{3+}$ composites were heated rapidly and uniformly by the cyclic MAM route. This classifies the method among simple and cost-effective ones and, evidently, the MAM technology is able to provide high yields with an easy scale-up as a viable alternative for the rapid synthesis of complex oxide composites[14].

The recorded EDS pattern, quantitative compositions, quantitative results and the SEM image of the synthesized $SPION/CaWO4:Er^{3+},Yb^{3+}$ composite are presented in Fig. 3. The EDS pattern shown in Fig. 3(a) displays that the $SPION/CaWO_4:Er^{3+},Yb^{3+}$ sample is composed of Fe, Ca, W, O, Er and Yb with the dominance of Fe, Ca, W, O. The EDS pattern and quantitative compositions in Fig. 3(a,b) could be well assigned to the $SPION/CaWO4:Er^{3+},Yb^{3+}$ composite. Thus, the incorporation of Fe_3O_4 nanoparticles to the $SPION/CaWO_4:Er^{3+},Yb^{3+}$ compound particles can be successfully achieved using the cyclic MAM reaction. The cyclic MAM reactions provide a convenient route for the synthesis of such complex products as $SPION/CaWO_4:Er^{3+},Yb^{3+}$ composites. The cyclic MAM route provides the exothermic energy to synthesize the bulk of the material uniformly, so that fine particles with controlled morphology can be fabricated in an environmentally friendly manner and without solvent waste generation.

(a)

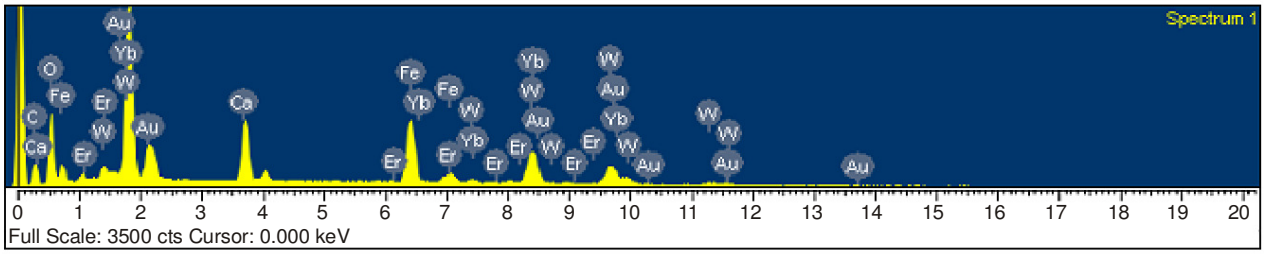

(b)

Spectrum	Instats.	C	O	Ca	Fe	Er	Yb	W	Au	Total
Spectrum1	Yes	9.83	22.95	6.36	15.09	1.38	1.19	31.97	10.94	100.00
Mean		9.83	22.95	6.36	15.09	1.38	1.49	31.97	10.94	100.00
Std. deviation		0.00	0.00	0.00	0.00	0.00	0.00	0.00	0.00	
Max.		9.83	22.95	6.36	15.09	1.38	1.49	31.97	10.94	
Min.		9.83	22.95	6.36	15.09	1.38	1.49	31.97	10.94	

(c)

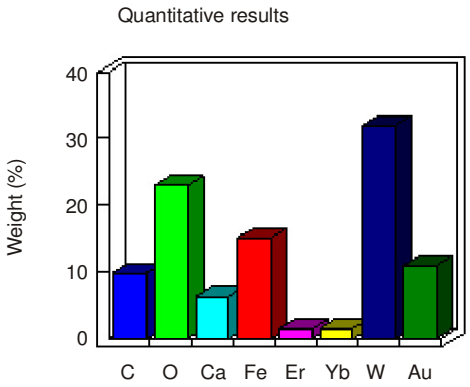

(d)

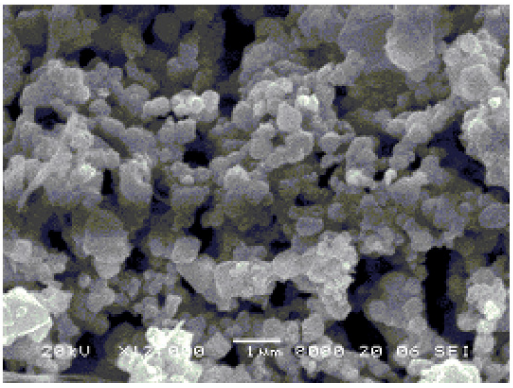

Fig. 3. (a) EDS pattern, (b) quantitative compositions, (c) quantitative results and (d) SEM image of the synthesized SPION/CaWO4: Er^{3+},Yb^{3+} composites

Fig. 4 shows the Raman spectra of the synthesized (a) $CaWO_4$ particles and (b) $CaWO_4$: Er^{3+}, Yb^{3+} (CWO:ErYb) and SPION/$CaWO_4$:Er^{3+},Yb^{3+} (F-CWO:ErYb) composites excited by the 514.5-nm line of an Ar-ion laser at 0.5 mW. The Raman spectra for the $CaWO_4$ particles in Fig. 4(a) were detected as $\nu_1(A_g)$, $\nu_3(B_g)$, $\nu_3(E_g)$, $\nu_4(E_g)$, $\nu_4(B_g)$ and $\nu_2(B_g)$ vibrations at 912, 838, 796, 399, 332 and 274 cm^{-1}, respectively, which provide evidence of a Scheelite structure. The well-resolved sharp peaks for the $CaWO_4$ particles indicate that the synthesized particles are highly crystallized. The vibration modes in the Raman spectrum of tungstates are classified into two groups, internal and external[15-17]. The internal vibrations are related to the $[WO_4]^{2-}$ molecular group with a stationary mass center. The external vibrations or lattice phonons are associated to the motion of the Ca^{2+} cation and rigid molecular units. The external modes were localized at 211-115 cm^{-1}. The internal modes for the $CaWO_4$:Er^{3+},Yb^{3+}(CWO:ErYb) and SPION/$CaWO_4$:Er^{3+},Yb^{3+}(F-CWO:ErYb) composites in Fig. 4(b) were detected as ν_1(Ag), ν_3(Bg), ν_3(Eg), ν_4(Eg), ν_4(Bg) and ν_2(Bg) vibrations at 911, 838, 796, 405, 342 and 313 cm^{-1}, respectively. The external modes were localized at 218-115 cm^{-1}. From the comparison in Fig. 4(b) it can be depicted that the peak positions are practically the same, while the intensities obtained from $CaWO_4$:Er^{3+},Yb^{3+} (CWO:ErYb) are slightly higher than those of SPION/$CaWO_4$:Er^{3+},Yb^{3+}(F-CWO:ErYb). The internal vibration mode frequencies are dependent on the lattice parameters and the degree of the partially covalent bonding between the cations and molecular ionic group[18-20] $[MoO_4]^{2-}$. Raman spectra of the synthesized $CaWO_4$: Er^{3+}, Yb^{3+}(CWO:ErYb) and SPION/$CaWO_4$:Er^{3+},Yb^{3+}(F-CWO:ErYb) composites indicate additional peaks at both middle (618, 577, 528 and 485 cm^{-1}) and lower frequencies (373, 355 and 269 cm^{-1}), which are attributed[19,21-24] to the doping ions of Er^{3+} and Yb^{3+}. It is noted that the Fe_3O_4 particles have no influence on the Raman spectra, while the doping ion of Er^{3+}/Yb^{3+} can influence the Raman spectra. Raman spectra proved that the Er^{3+}/Yb^{3+} doping ions can influence the structure of the host materials.

Conclusion

The SPION/$CaWO_4$:Er^{3+},Yb^{3+} composites were successfully synthesized by the cyclic MAM method. The microstructure exhibited a well-defined and homogeneous morphology with the B$CaWO_4$:Er^{3+},Yb^{3+} and Fe_3O_4 particle size of 1-2 and 0.1-0.5 μm, respectively. The Fe_3O_4 nanoparticles were self-preferentially crystallized and immobilized on the surface of $CaWO_4$:Er^{3+},Yb^{3+} particles. The Raman spectra of the synthesized $CaWO_4$:Er^{3+},Yb^{3+}(CWO:ErYb) and SPION/$CaWO_4$:

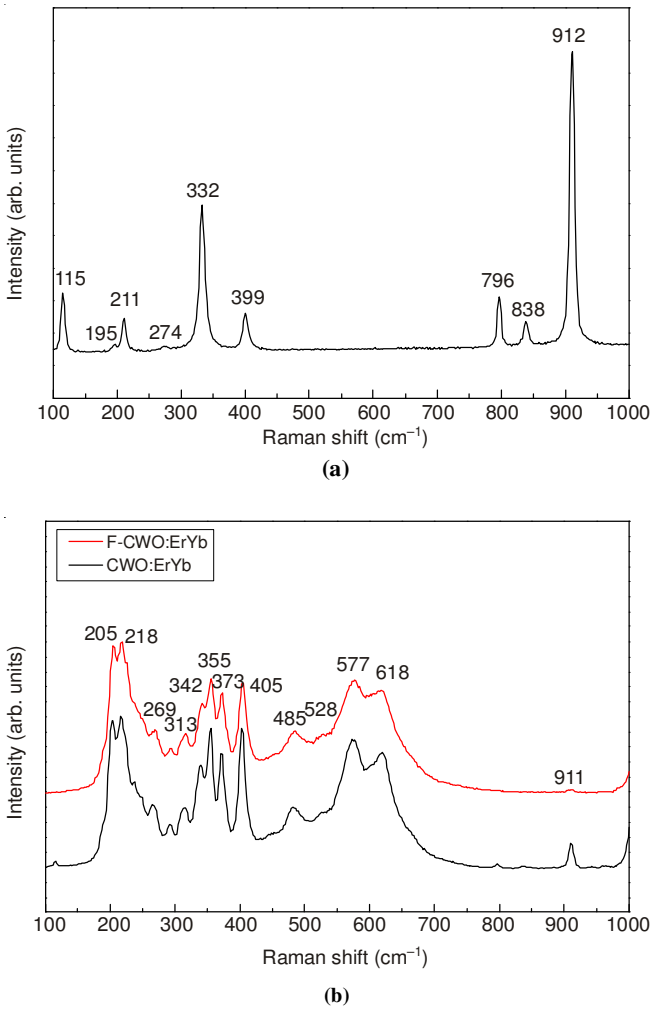

Fig. 4. Raman spectra of the synthesized (a) $CaWO_4$ particles and (b) $CaWO_4$:Er^{3+},Yb^{3+}(CWO:ErYb) and SPION/$CaWO_4$:Er^{3+},Yb^{3+}(F-CWO:ErYb) composites

Er^{3+},Yb^{3+}(F-CWO:ErYb) composites indicate additional peaks at both middle (618, 577, 528 and 485 cm^{-1}) and lower frequencies (373, 355 and 269 cm^{-1}), which are attributed to the doping ions of Er^{3+} and Yb^{3+}.

ACKNOWLEDGEMENTS

This study was supported by Basic Science Research Program through the National Research Foundation of Korea (NRF) funded by the Ministry of Education, Science and Technology (2013-054508).

REFERENCES

1. D. Liu, L. Tong, J. Shi and H. Yang, *J. Alloys Comp*., **512**, 361 (2012).
2. L. Liu, L. Xiao and H.Y. Zhu, *Chem. Phys. Lett*., **539-540**, 112 (2012).
3. Q. Wang, X. Yang, L. Yu and H. Yang, *J. Alloys Comp*., **509**, 9098 (2011).
4. J.H. Ryu, G.S. Park, K.M. Kim, C.S. Lim, J.-W. Yoon and K.B. Shim, Appl. Phys., *A Mater. Sci. Process*., **88**, 731 (2007).
5. H. Wu, Y. Hu, F. Kang, L. Chen, X. Wang, G. Ju and Z. Mu, *Mater. Res. Bull*., **46**, 2489 (2011).
6. G.H. Lee and S. Kang, *J. Lumin*., **131**, 2606 (2011).
7. F.B. Cao, L.S. Li, Y.W. Tian, Y.J. Chen and X.R. Wu, *Thin Solid Films*, **519**, 7971 (2011).
8. J. Liao, B. Qiu, H. Wen, J. Chen, W. You and L. Liu, *J. Alloys Comp*., **487**, 758 (2009).
9. Y. Zheng, Y. Huang, M. Yang, N. Guo, H. Qiao, Y. Jia and H. You, *J. Lumin*., **132**, 362 (2012).
10. M. Sadegh, A. Badiei, A. Abbasi, H. Goldooz and G. Mohammadi Ziarani, *J. Lumin*., **130**, 2072 (2010).
11. W. Wang, P. Yang, S. Gai, N. Niu, F. He and J. Lin, *J. Nanopart. Res*., **12**, 2295 (2010).
12. Y. Tian, Y. Liu, R. Hua, L. Na and B. Chen, *Mater. Res. Bull*., **47**, 59 (2012).
13. C.S. Lim, *Mater. Chem. Phys*., **131**, 714 (2012).
14. C.S. Lim, *J. Lumin*., **132**, 1774 (2012).
15. T.T. Basiev, A.A. Sobol, Y.K. Voronko and P.G. Zverev, *Opt. Mater*., **15**, 205 (2000).
16. T.T. Basiev, A.A. Sobol, P.G. Zverev, L.I. Ivleva, V.V. Osiko and R.C. Powell, *Opt. Mater*., **11**, 307 (1999).
17. D. Rangappa, T. Fujiwara, T. Watanabe and M. Yoshimura, *J. Electroceram*., **17**, 853 (2006).
18. V.V. Atuchin, T.A. Gavrilova, V.G. Kostrovsky, L.D. Pokrovsky and I.B. Troitskaia, *Inorg. Mater*., **44**, 622 (2008).
19. V.V. Atuchin, O.D. Chimitova, T.A. Gavrilova, M.S. Molokeev, S.J. Kim, N.V. Surovtsev and B.G. Bazarov, *J. Cryst. Growth*, **318**, 683 (2011).
20. V.V. Atuchin, T.A. Gavrilova, T.I. Grigorieva, N.V. Kuratieva, K.A. Okotrub, N.V. Pervukhina and N.V. Surovtsev, *J. Cryst. Growth*, **318**, 987 (2011).
21. C.S. Lim, *Mater. Res. Bull*., **47**, 4220 (2012).
22. V.V. Atuchin, V.G. Grossman, S.V. Adichtchev, N.V. Surovtsev, T.A. Gavrilova and B.G. Bazarov, *Opt. Mater*., **34**, 812 (2012).
23. C.S. Lim, *Mater. Res. Bull*., **48**, 3805 (2013).
24. C.S. Lim, *Mater. Chem. Phys*., **140**, 154 (2013).